

Evolution of collectivity near mid-shell from excited-state lifetime measurements in rare earth nuclei

V. Werner,^{1,2,*} N. Cooper,¹ J.-M. Régis,³ M. Rudigier,^{3,4} E. Williams,^{1,†} J. Jolie,³ R. B. Cakirli,⁵ R. F. Casten,¹ T. Ahn,^{1,6} V. Anagnostatou,^{1,4} Z. Berant,^{1,7} M. Bonett-Matiz,¹ M. Elvers,^{1,3} A. Heinz,^{1,8} G. Ilie,¹ D. Radeck,^{1,3} D. Savran,^{1,9,10} and M. K. Smith^{1,6}

¹*Wright Nuclear Structure Laboratory, Yale University, P.O. Box 208120, New Haven, Connecticut 06520, USA*

²*Institut für Kernphysik, Technische Universität Darmstadt, Schlossgartenstr. 9, 64289 Darmstadt, Germany*

³*Institut für Kernphysik, Universität zu Köln, Zùlpicher Str. 77, 50937 Köln, Germany*

⁴*University of Surrey, Guildford, Surrey, GU2 7XH, United Kingdom*

⁵*Department of Physics, University of Istanbul, 34134 Istanbul, Turkey*

⁶*Physics Department, University of Notre Dame, 225 Nieuwland Science Hall, Notre Dame, Indiana 46656*

⁷*Nuclear Research Center Negev, Beer-Sheva 84190, Israel*

⁸*Department of Fundamental Physics, Chalmers University of Technology, SE-412 96 Göteborg, Sweden*

⁹*ExtreMe Matter Institute EMMI and Research Division, GSI Helmholtzzentrum für Schwerionenforschung, D-64291 Darmstadt, Germany*

¹⁰*Frankfurt Institute for Advanced Studies (FIAS), D-60438 Frankfurt am Main, Germany*

(Received 3 August 2015; revised manuscript received 26 December 2015; published 18 March 2016)

The $B(E2)$ excitation strength of the first excited 2^+ state in even-even nuclei should directly correlate with the size of the valence space and maximize at mid-shell. A previously found saturation of $B(E2)$ strengths in well-deformed rotors at mid-shell is tested through high-precision measurements of the lifetimes of the lowest-lying 2^+ states of the ^{168}Hf and ^{174}W rare earth isotopes. Measurements were performed using fast LaBr_3 scintillation detectors. Combined with the recently remeasured $B(E2; 2_1^+ \rightarrow 0_1^+)$ values for Hf and W isotopes the new data remove discrepancies observed in the differentials of $B(E2)$ values for these isotopes.

DOI: [10.1103/PhysRevC.93.034323](https://doi.org/10.1103/PhysRevC.93.034323)

I. INTRODUCTION

Properties of the first excited 2^+ state in even-even nuclei, such as excitation energy and $E2$ excitation strength, are often used as measures for the degree of collectivity at low excitation energies and are, therefore, benchmarks for nuclear models. In particular, the $B(E2)$ reduced transition probability is a direct probe for the wave functions of the lowest-lying states. In general, away from closed magic shells one finds enhanced collectivity, which is manifested in large axially symmetric deformations. Such a region is found in mass $A \approx 170$ rare earth nuclei, where typical β deformation values are about 0.2–0.3. This directly translates into large $B(E2)$ values, of the order of a few hundreds of Weisskopf units, due to the geometrical relation between β and $B(E2)$ strength. Typical excitation energies of 2_1^+ states near mid-shell are of the order of 100 keV, and typical lifetimes are of the order of a nanosecond.

In a simple collective picture, neglecting individual nuclear orbitals and considering only a single- j shell for an isotopic chain, $B(E2)$ strengths should rise monotonically toward, and maximize at, mid-shell. This trend can also be found in the collective SU(3) limit of the interacting boson model (IBM) [1], where

$$B(E2; 0_1^+ \rightarrow 2_1^+) = e_B^2 \cdot N(2N + 3), \quad (1)$$

with the number of bosons N and the effective boson charge e_B . However, a saturation of $B(E2; 0_1^+ \rightarrow 2_1^+)$ strengths around mid-shell has recently been recognized in the rare earth region from available data [2], where the slope of $B(E2)$ strength versus neutron number toward mid-shell was strongly reduced from the quadratic expression in Eq. (1) (see Fig. 1 in Ref. [2]). The same (inverted) effect has been observed in g factors of the 2_1^+ states in this region [3]. Qualitatively, this saturation has been argued [2] to arise from the overlaps of proton and neutron wave functions: as neutrons fill different l_j orbitals than protons near mid-shell, wave function overlaps and, hence, collectivity, do not increase as a function of valence neutron number as in Eq. (1). Within the IBM, this has effectively been incorporated by considering fractional filling of the shell, and a more microscopic approach within the projected shell model [4] led to similar conclusions.

However, recent measurements of 2_1^+ lifetimes in the Hf and W isotopes [5–8] found large discrepancies from literature values and gave rise to the need for new, high-precision measurements of the lifetimes involved. In the present work, we measured 2_1^+ lifetimes in the isotopes ^{168}Hf and ^{174}W using the fast timing technique with $\text{LaBr}_3(\text{Ce})$ scintillators. With these new lifetime results, both $B(E2)$ values and differential $B(E2)$ values are extracted. If there is a saturation in $B(E2)$ values in deformed nuclei, differentials of $B(E2)$ values are expected to be smooth and small. The differential results using the old and new $B(E2)$ values are discussed in Sec. IV.

II. EXPERIMENTAL TECHNIQUE

The experiment was performed using the moving tape collector [9] at the Wright Nuclear Structure Laboratory (WNSL)

*vw@ikp.tu-darmstadt.de

†Present address: Department of Nuclear Physics, Research School of Physics and Engineering, Australian National University, Canberra, Australian Capital Territory 2601, Australia.

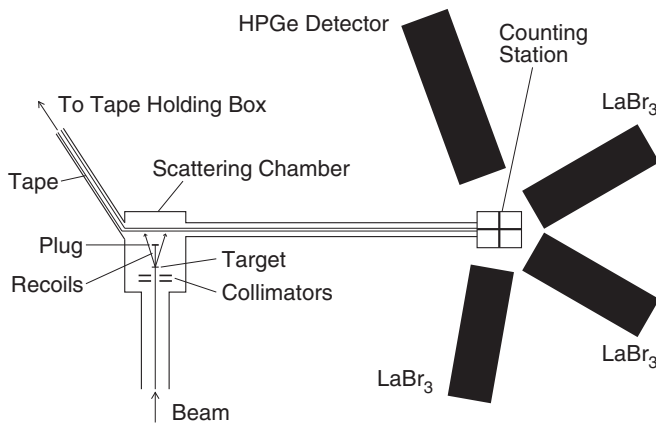


FIG. 1. Schematic top view of the setup at the moving tape collector. Three LaBr₃ detectors were placed in a close geometry around the source position. Activity was moved from the scattering chamber to the counting station by a plastic tape. In addition, an HPGe detector was used in order to obtain a high-resolution spectrum.

of Yale University. The reactions $^{169}\text{Tm}(^{12}\text{C}, 7n)^{174}\text{Re}$ and $^{159}\text{Tb}(^{16}\text{O}, 7n)^{168}\text{Ta}$ were used at 115- and 130-MeV beam energies, respectively, to produce the β -decay parents of ^{174}W and ^{168}Hf . The beams were delivered by the 20-MV ESTU tandem accelerator at the WNSL. Recoils from the target were implanted on a tape, whereas the unreacted beam was stopped in a gold plug arranged between the target and the tape. The tape was moved in cycles of approximately 2.5 times the half-lives of the respective decay parents, so that the activation was placed in the center of the detector array and overall count rates for the desired β -decay products were optimized. The γ -rays emitted after β decay were detected by three 1.5-in. \times 1.5-in. LaBr₃ scintillators, shielded from the activation chamber, so that target activation and decay measurement were carried out simultaneously. Residual activity was removed from the setup to a tape holding box. An HPGe detector was used in addition

to the scintillators, to ensure that no contaminant γ transitions were present in the vicinity of the transitions of interest. A schematic of the setup is shown in Fig. 1.

Scintillator time signals were fed into three time-to-analog converters (TACs), such that each detector served as a start or stop signal, resulting in six independent start-stop combinations. The TACs were calibrated with well-known cable delays in steps of 2 ns. The TAC output was recorded in a standard analog-to-digital converter in the WNSL data acquisition system, where individual energy and time information was also recorded. The energy resolution of the LaBr₃ scintillators (3% at ^{60}Co energies) allowed one to reliably carry out background subtraction, e.g., from Compton scattered γ rays or room background.

According to the scheme shown in Fig. 2 for data from the calibration standard ^{152}Sm , used here, gates were set on the $4_1^+ \rightarrow 2_1^+$ and $2_1^+ \rightarrow 0_1^+$ transitions in each detector, and time differences between each pair of detectors were projected. In addition, three sets of background gates were defined and normalized to the full energy gates, as follows: (i) gates on the $4_1^+ \rightarrow 2_1^+$ transition and above the $2_1^+ \rightarrow 0_1^+$ transition; (ii) gates above the $4_1^+ \rightarrow 2_1^+$ transition and on the $2_1^+ \rightarrow 0_1^+$ transition; and (iii) gates above both transition energies. Background gates were taken above the transitions of interest to avoid gating on their respective Compton events. Due to the lifetimes of higher-lying states, their Compton events underneath and next to the transitions of interest have an effective lifetime that needs to be corrected for. Therefore, time difference spectra Bg1 and Bg2 (see Fig. 2) were subtracted from the raw spectrum resulting from the full energy gates. Since both Bg1 and Bg2 contain “background-background” coincidences, the corresponding time difference spectrum Bg3 had to be added back in.

This gating procedure was analogously performed for the measurements on ^{168}Hf and ^{174}W . Since background windows did not always have exactly the widths of the gates on the transitions of interest, the resulting spectra were

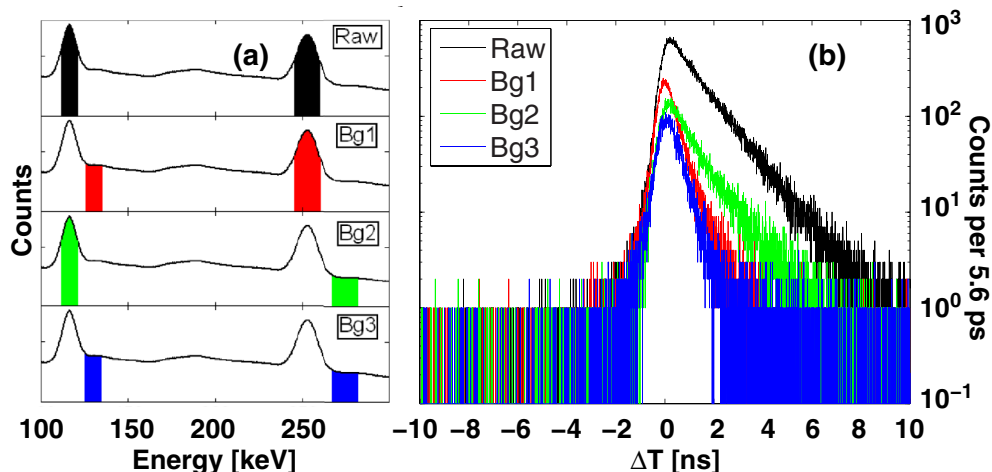


FIG. 2. Schematic of the gating procedure for the example of the $2_1^+ \rightarrow 0_1^+$ (121.8-keV) and $4_1^+ \rightarrow 2_1^+$ (244.7-keV) transitions in ^{152}Sm , after decay from ^{152}Eu . (a) Regions where background and full energy gates were set in a projected LaBr₃ detector spectrum. (b) Resulting time difference spectra for each gate combination. The lowest (blue) spectrum corresponds to almost-prompt background from higher-lying states.

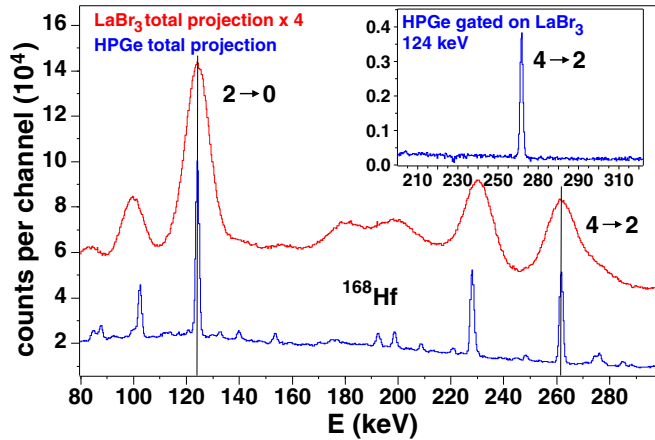


FIG. 3. Projections of HPGe (blue line) and LaBr₃ (red line; multiplied by 4 for visibility) from $\gamma\gamma$ coincidences among all three HPGe-LaBr₃ detector pairs from the ^{168}Hf experiment. Transitions of interest are marked. Inset: Background-corrected HPGe spectrum, gated on the $2_1^+ \rightarrow 0_1^+$ transition in the LaBr₃ detectors. No potential contaminant transitions appear.

scaled accordingly. Figures 3 and 4 show sample spectra obtained from the collected coincidence data. Total projections of HPGe-LaBr₃ matrices (summed up for all three LaBr₃ detectors) are shown on top of each other and the relevant transitions of interest are marked. Within the line profiles of the $4_1^+ \rightarrow 2_1^+$ or $2_1^+ \rightarrow 0_1^+$ transitions some structure is visible in the HPGe spectra. Gating on the $2_1^+ \rightarrow 0_1^+$ transition of ^{168}Hf in the LaBr₃ detectors results in the HPGe spectrum shown in the inset in Fig. 3, and no contaminant transition is present in this case.

For ^{174}W , after following the same procedure, a small contaminant transition is visible at about 240 keV after gating on the $2_1^+ \rightarrow 0_1^+$ transition in the LaBr₃ detectors. Similarly, a

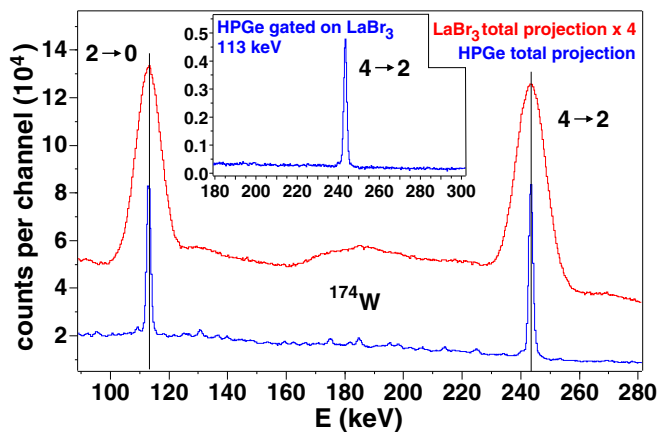


FIG. 4. Projections of HPGe (blue line) and LaBr₃ (red line; multiplied by 4 for visibility) from $\gamma\gamma$ coincidences among all three HPGe-LaBr₃ detector pairs from the ^{174}W experiment. Transitions of interest are marked. Inset: Background-corrected HPGe spectrum, gated on the $2_1^+ \rightarrow 0_1^+$ transition in the LaBr₃ detectors. Contaminant coincident transitions from ^{176}W are visible at 109 and 240 keV.

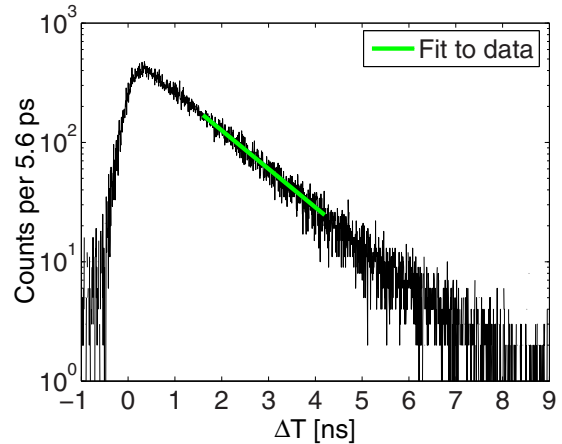


FIG. 5. Logarithmic plot of the time difference spectrum for the decay of the 2_1^+ state in ^{174}W after random subtraction. The green line indicates the line fit (see text) to the linearly down-sloping part of the spectrum.

gate on the FWHM of the $4_1^+ \rightarrow 2_1^+$ transition reveals a small peak at about 109 keV, which can be seen in the total HPGe projection in Fig. 4. This coincidence is known between the $4_1^+ \rightarrow 2_1^+$ and the $2_1^+ \rightarrow 0_1^+$ transitions in ^{176}W , which may occur β -delayed from production of ^{176}Re in the reaction used. The influence on the lifetime measurement is discussed in the following section.

III. RESULTS

A simple line fit has been applied to the slope of the logarithmic time difference data. The most appropriate and reliable region for the fit was selected by moving a gate a few hundred picoseconds wide across the time difference spectra and fitting a line. Only the region that resulted in a constant slope, and, hence, did not show any effects of the prompt peak or background, was used to obtain the final result. A sample fit is shown for the example of ^{174}W in Fig. 5. This procedure has been followed for each of the six available detector combinations. The results of the line fits which yield the 2_1^+ lifetimes of ^{168}Hf and ^{174}W for all detector pairs are shown in Fig. 6. The individual detector pairs yielded consistent results for each case; these results were then combined using an error-weighted average. In the case of the tungsten experiment, only five pairs of detectors could be used.

The contaminant coincidence intensity from ^{176}W in the ^{174}W measurement amounts to about 5% of the coincidence intensity of interest in ^{174}W . The 2_1^+ lifetime in ^{176}W is known to be 1.431(9) ns [6]. This differs by less than 100 ps from the lifetime obtained from the present data and the systematic error induced by the contaminant coincidence is estimated to be below 5 ps. Nevertheless, gates were set only on the right halves of the $2_1^+ \rightarrow 0_1^+$ and $4_1^+ \rightarrow 2_1^+$ transitions in ^{174}W , eliminating any potential influence from the contaminant. The background next to the respective peaks is not really the same as the background underneath the peaks, which is another source of potential systematic error. On the basis of choosing

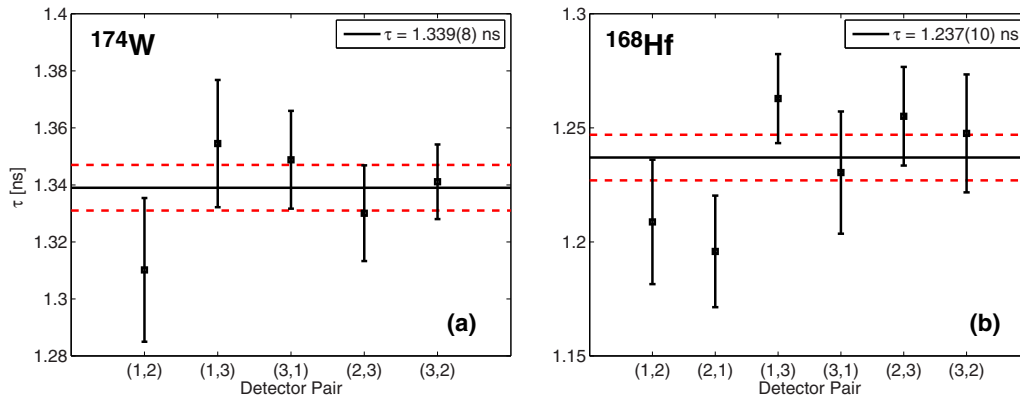


FIG. 6. Lifetimes obtained from individual detector pairs for the 2_1^+ state in (a) ^{174}W and (b) ^{168}Hf . The solid black line indicates the weighted averages, and the dashed red lines correspond to the standard deviations of the averages. The given errors of the averages are statistical errors only.

different background regions we conservatively estimate this systematic error to about 0.5%.

The experiment yields new lifetimes for the first excited 2^+ states of ^{168}Hf and ^{174}W , with considerably reduced error bars compared to literature data. For ^{168}Hf , the new result of $\tau(2_1^+; ^{168}\text{Hf}) = 1.237(10)(7)$ ns is in agreement with the adopted literature value [10] of 1.28(6) ns. Note that the first error represents the statistical error, and the second represents the systematic error. For ^{174}W , however, the new value of $\tau(2_1^+; ^{174}\text{W}) = 1.339(8)(7)$ ns is about 20% lower than the adopted literature value of 1.64(10) ns [11]. Similar deviations have been found in previous work on other Hf and W isotopes [7,8]. Modifications to known data of the order of 20% should be taken seriously, especially in view of the qualitative and quantitative arguments relating to a $B(E2)$ saturation near mid-shell. Using the lifetimes from the present work, the new $B(E2)$ values, along with existing data, are listed in Table I. One clearly sees a peaking of the $B(E2)$ values prior to midshell ($N = 104$), in contrast to simple models. Most striking is the rapid rise of $B(E2; 2_1^+ \rightarrow 0_1^+)$ values from the literature value [19,20] at $N = 96$ to the recent result [7] at $N = 98$, by about 30%, in the W isotopic chain. The sudden rise in $B(E2)$ values at $N = 98$ is followed by a near-linear decrease towards higher neutron numbers. We note that the recoil distance methods used to obtain the 2_1^+ lifetimes in Refs. [19,20] are prone to systematic error, potentially leading to an overestimate of its lifetime.

IV. DISCUSSION

The presently measured $B(E2; 2_1^+ \rightarrow 0_1^+)$ value for ^{174}W , combined with recent results on several other Hf and W isotopes, resolve a puzzling anomaly and shed light on the evolution of collectivity in this region. In Ref. [21] it was shown that while plots of various characteristic observables such as $E(2_1^+)$, $R_{4/2}$, S_{2n} , charge radii, and $B(E2)$ values can be individually simple, the patterns for each of these observables differ among themselves since they depend in different ways on structure. For example, as collectivity grows and deformation sets in as a function of the neutron number, $E(2_1^+)$ decreases while $R_{4/2}$ increases. Likewise, the yrast $B(E2)$ values increase while the two-neutron separation energy S_{2n} decreases. However, it was shown in [21] that differentials of these observables behave very similarly to each other, and in characteristic ways across a region, to the extent that knowledge of the behavior of one differential can even be used to guide estimates of others. In Ref. [21] data for several mass regions were inspected. Despite the smooth overall behavior of these differentials in most ranges of nucleon numbers, a few anomalies were noted. One of the most striking was in the $B(E2)$ values in the upper end of the $Z = 50\text{--}82$, $N = 82\text{--}126$ major shell region—in particular, in the Hf and W isotopes.

The point is illustrated in Fig. 7(a), based on Ref. [21]. There is a smooth overall trend in the $B(E2)$ differentials in the heavier isotopes ($N > 108$ in W to Pb), as shown in Ref. [21],

TABLE I. $B(E2; 2_1^+ \rightarrow 0_1^+)$ values used in the discussion. Entries in boldface are new values since Ref. [21], including those in the present work for ^{168}Hf and ^{174}W .

	$B(E2; 2_1^+ \rightarrow 0_1^+)$ value (W.u.)								
	$N = 90$	$N = 92$	$N = 94$	$N = 96$	$N = 98$	$N = 100$	$N = 102$	$N = 104$	$N = 106$
^{72}Hf	51(7) [12]	68(10) [13]	128(7) [14]	160.4(16)^a	181(6) [5] ^b	194(6) [8]	199(6) [8]	182(7) [8]	160(3) [15]
^{74}W			117(6) [16]	124(3) [17]	189(6) [7]	166.9(14)^a	168(1) [6]	153(2) [7]	140(6) [18]

^aFrom this work.

^bThis value, from Ref. [5], was inadvertently omitted in Ref. [21].

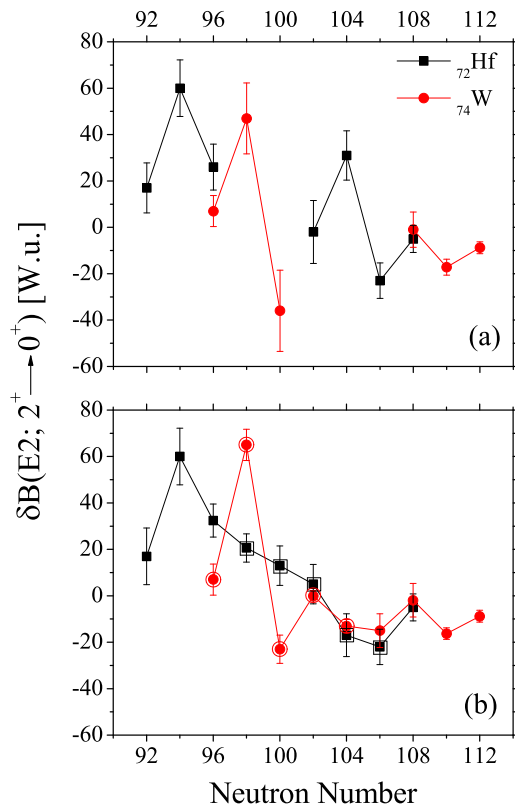


FIG. 7. (a) $\delta B(E2; 2_1^+ \rightarrow 0_1^+)$ values for Hf and W isotopes using the old data (from Ref. [21], which accidentally excluded the value from Ref. [5] for ^{170}Hf), and (b) using that value, the values from this work and from Refs. [6–8]. These recent data are marked by open symbols.

but there are striking oscillations as well as gaps in the data in Hf and in the lighter W isotopes, shown in Fig. 7(a). Since a given $B(E2)$ value occurs twice in the differential, once with a positive sign and once with a negative sign, such oscillations often point to incorrect experimental values. It was speculated in Ref. [21] either that the light Hf-W data were not correct or that there was some significant and difficult-to-understand anomalous underlying physics. The present data and other measurements by the Cologne group since 2010 [6–8] now allow one to fill in the missing values and correct some previous results, resolving the dilemma. Figure 7(b) shows the same region with the new Hf and W $B(E2)$ differentials.

For Hf, the oscillations in the earlier data are now replaced by a smooth upward trend with decreasing neutron number, along with a sharp drop for the lowest neutron number where data are available. Bear in mind that, since the differentials are

defined as $\delta B(E2) = B(E2)_N - B(E2)_{N-2}$, positive values mean that the $B(E2)$ values increase with increasing neutron number, and vice versa. Thus, the trend in Hf isotopes with increasing neutron number reflects a strong increase in $B(E2)$ values between $N = 92$ and $N = 94$, followed by a slowing of that increase toward mid-shell at $N = 104$ and a decrease thereafter. This is precisely the expected behavior for this collective observable across a major shell region, whereas oscillations in the older data were very difficult to understand. The recent $B(E2)$ data for $^{176,178}\text{W}_{102,104}$ eliminate the gap in Fig. 7(a) from $N = 100$ to $N = 108$ and the differentials are nearly constant at about -10 W.u. from $N = 100$ until $N = 112$; that is, the $B(E2)$ values slightly but systematically decrease with N starting already well below the geometrical mid-shell point. In a single- j shell the $B(E2)$ values should peak at mid-shell, but this is not necessarily the case in major shell regions, where several orbits come into play and where their distribution in j values is asymmetric, with high j values dominating early in the shell. A microscopic calculation is called for to understand the observed peaking below mid-shell in W, which has similarly been observed in the Os isotopic chain [22]. The sharp increase in $\delta B(E2)$ for $N = 98$ reflects the suddenly low $B(E2)$ value of 124 W.u. at $N = 96$ (^{170}W). With respect to the discussion in the previous section, a remeasurement of this value using techniques similar to those in the present work would be worthwhile.

V. SUMMARY

Fast-timing lifetime measurements of the 2_1^+ states of ^{168}Hf and ^{174}W were made using LaBr₃ detectors following β decay of the parent nuclei produced in fusion evaporation reactions. The uncertainties in the lifetimes are about an order of magnitude smaller than in previous measurements. The ^{168}Hf result confirms the previous value, while the ^{174}W lifetime [and hence the $B(E2; 2_1^+ \rightarrow 0_1^+)$ value] is about 20% different. These values, combined with other recent measurements by the Cologne group, substantially alter the observed evolution of collectivity near mid-shell in these elements and confirm its saturation prior to mid-shell in W. An analysis in terms of differentials of $B(E2)$ values resolves previously noted, unexplained anomalies and reveals a smoother systematics than previously thought.

ACKNOWLEDGMENTS

This work was supported by the US DOE under Grant No. DE-FG02-91ER40609 and by the German DFG under Grant Nos. SFB 634 and Jo391/16-1. R.B.C. acknowledges support from the Max-Planck Partner group and Istanbul University Scientific Research Project No. 26435.

- [1] F. Iachello and A. Arima, *The Interacting Boson Model* (Cambridge University Press, Cambridge, UK, 1987).
 [2] J. Y. Zhang, R. F. Casten, A. Wolf, Z. Berant, R. B. Cakirli, N. V. Zamfir, and E. A. McCutchan, *Phys. Rev. C* **73**, 037301 (2006).

- [3] Z. Berant, A. Wolf, N. V. Zamfir, M. A. Caprio, D. S. Brenner, N. Pietralla, R. L. Gill, R. F. Casten, C. W. Beausang, R. Krücken, C. J. Barton, J. R. Cooper, A. A. Hecht, D. M. Johnson, J. R. Novak, H. Cheng, B. F. Albanna, and G. Gürdal, *Phys. Rev. C* **69**, 034320 (2004).

- [4] B.-A. Bian, Y.-M. Di, G.-L. Long, Y. Sun, J. Y. Zhang, and J. A. Sheikh, *Phys. Rev. C* **75**, 014312 (2007).
- [5] A. Costin, T. Ahn, B. Bochev, K. Dusling, T. C. Li, N. Pietralla, G. Rainovski, and W. Rother, *Phys. Rev. C* **74**, 067301 (2006).
- [6] J.-M. Régis, Th. Materna, S. Christen, C. Bernards, N. Braun, G. Breuer, Ch. Fransen, S. Heinze, J. Jolie, T. Meersschat, G. Pascovici, M. Rudigier, L. Steinert, S. Thiel, N. Warr, and K. O. Zell, *Nucl. Inst. Methods A* **606**, 466 (2009).
- [7] M. Rudigier, J.-M. Régis, J. Jolie, K. O. Zell, and C. Fransen, *Nucl. Phys. A* **847**, 89 (2010).
- [8] M. Rudigier, K. Nomura, M. Dannhoff, R.-B. Gerst, J. Jolie, N. Saed-Samii, S. Stegemann, J.-M. Régis, L. M. Robledo, R. Rodríguez-Guzmán, A. Blazhev, Ch. Fransen, N. Warr, and K. O. Zell, *Phys. Rev. C* **91**, 044301 (2015).
- [9] N. V. Zamfir and R. F. Casten, *J. Res. Natl. Inst. Stand. Technol.* **105**, 147 (2000).
- [10] C. M. Baglin, *Nucl. Data Sheets* **111**, 1807 (2010).
- [11] E. Browne and H. Junde, *Nucl. Data Sheets* **87**, 15 (1999).
- [12] L. Weissman, M. Hass, and C. Broude, *Phys. Rev. C* **57**, 621 (1998).
- [13] B. Singh, *Nucl. Data Sheets* **93**, 243 (2001).
- [14] B. Bochev, S. Iliev, R. Kalpakchieva, S. A. Karamian, T. Kutsarova, E. Nadjakov, and Ts. Venkova, *Nucl. Phys. A* **282**, 159 (1977).
- [15] E. Achterberg, O. A. Capurro, and G. V. Marti, *Nucl. Data Sheets* **110**, 1473 (2009).
- [16] G. D. Dracoulis, G. D. Sprouse, O. C. Kistner, and M. H. Rafailovich, *Phys. Rev. C* **29**, 1576 (1984).
- [17] C. Michel, Y. El Masri, R. Holzmann, M. A. Van Hove, and J. Vervier, *Z. Phys. A* **298**, 213 (1980).
- [18] E. A. Mccutchan, *Nucl. Data Sheets* **126**, 151 (2015).
- [19] M. N. Rao, N. R. Johnson, F. K. McGowan, I. Y. Lee, C. Baktash, M. Oshima, J. W. McConnell, J. C. Wells, A. Larabee, L. L. Riedinger, R. Bengtsson, Z. Xing, Y. S. Chen, P. B. Semmes, and G. A. Leander, *Phys. Rev. Lett.* **57**, 667 (1986).
- [20] F. K. McGowan, N. R. Johnson, I. Y. Lee, C. Baktash, J. W. McConnell, M. N. Rao, M. Oshima, J. C. Wells, A. Larabee, L. L. Riedinger, R. Bengtsson, and Z. Xing, *Nucl. Phys. A* **530**, 490 (1991).
- [21] R. B. Cakirli, R. F. Casten, and K. Blaum, *Phys. Rev. C* **82**, 061306R (2010).
- [22] C. B. Li, X. G. Wu, X. F. Li, C. Y. He, Y. Zheng, G. S. Li, S. H. Yao, S. P. Hu, H. W. Li, J. L. Wang, J. J. Liu, C. Xu, J. J. Sun, and W. W. Qu, *Phys. Rev. C* **86**, 057303 (2012).